

# Interpretation of impedance spectroscopy of cement paste via computer modelling

## Part I *Bulk conductivity and offset resistance*

R. T. COVERDALE, B. J. CHRISTENSEN, H. M. JENNINGS\*, T. O. MASON  
*Department of Materials Science and Engineering, and \*Department of Civil Engineering,  
Northwestern University, Evanston, IL 60208, USA*

D. P. BENTZ, E. J. GARBOCZI  
*National Institute of Standards and Technology, Building Materials Division, Building 226,  
Room 348 B, Gaithersburg, MD 20899, USA*

Computer simulation of impedance spectroscopy (IS) of hydrating cement paste, using a three-dimensional, four-phase model, is described. Two puzzling features of experimental IS results, the possible offset resistance in the Nyquist plot and the sharp decrease in normalized conductivity within the first 50 h of reaction, have been studied using the computer simulation model. Insight is provided into these features using the ability of the model to compare quantitatively microstructure and properties. It is concluded that the offset resistance is an experimental artefact, and does not directly relate to microstructure. The drop in conductivity during the first 50 h is shown to be a consequence of a gradual shift from parallel-dominated to series-dominated behaviour of the electrical conductivity, as microstructural modifications take place during hydration, causing the capillary pore structure to become more tortuous. This tortuosity can also explain the high-frequency impedance behaviour in terms of a two-arc response.

### 1. Introduction

Portland cement paste is a porous, chemically bonded ceramic which results from the reaction of an initial suspension of Portland cement powder and water. Portland cement is a manufactured material, consisting primarily of calcium silicates, with fairly minor amounts of aluminates, ferrites, and sulphates [1]. The hydration reaction between cement and water in time produces a multi-phase, rigid material. After initial mixing, the water originally between the cement particles gradually becomes a highly conductive pore fluid, due to the dissolution of calcium and alkali ions from the cement. The main product of reaction is a poorly crystalline or amorphous calcium silicate hydrate commonly referred to as C–S–H (standard cement chemistry notation: C = CaO, S = SiO<sub>2</sub>, and H = H<sub>2</sub>O), with the hyphens denoting a varying C/S ratio non-stoichiometric compound. This phase is also conductive, because its nanometre-sized pores are filled with conductive pore fluid. Another important product is calcium hydroxide, CH, which forms in crystals and is an insulator. Because the total reaction products have a higher specific volume than the reactants (cement and water), the volume originally containing the pore fluid, termed capillary porosity, is reduced and becomes increasingly tortuous. The capillary pores control properties such as permeability,

strength, toughness, and durability. With respect to electrical properties, on which this paper focuses, the only phases of importance are capillary porosity and C–S–H. Other phases are insulators [2].

Analysis of porosity by methods such as scanning electron microscopy (SEM) or gas adsorption, is complicated by the fact that the high vacuum necessary for these measurements removes water, which is an integral part of the cement paste structure. Recently, impedance spectroscopy (IS) [3] has been used to study the microstructure of cement paste [4–12]. IS, as it is commonly practiced, is a technique in which an alternating voltage at a single frequency is applied to a sample, and the magnitude and phase of the current measured [3]. Impedance spectra are then given by the behaviour of the impedance (or other quantities derived from the impedance and the frequency [3]) as a function of frequency. It has been shown that the impedance spectra of cement pastes depend strongly on the amount of porosity present in the microstructure, and, perhaps more importantly, on the arrangement and connectivity of the porosity [2]. By studying the impedance response at different times during the reaction, information about the arrangement and interconnectivity of the microstructure in the undried state can be obtained.

It is very common to study the cement paste made from pure tricalcium silicate ( $C_3S$ ) and water, because  $C_3S$  is the major component of Portland cement. This reaction serves as a useful, somewhat simpler approximation for the hydration of Portland cement. However, the electrical properties of  $C_3S$  paste are qualitatively very similar to Portland cement paste, because both capillary porosity and C-S-H are still the main phases. Fig. 1 shows an impedance curve of a tricalcium silicate paste. The impedance curve is in the form of a Nyquist plot [3], with  $-Z''$  plotted against  $Z'$ , and where  $Z''$  and  $Z'$  are the imaginary and real parts, respectively, of the impedance  $Z$ . Applied frequency parameterizes the plot, with frequency increasing from right to left in Fig. 1. The paste was mixed with an initial weight ratio of water to cement (denoted  $w/c$ ) of 0.45, and was reacted for 14 days. The degree of hydration or reaction,  $\alpha$ , is defined as the fraction of cement that has hydrated. The impedance curve in Fig. 1 exhibits a large electrode arc on the low-frequency (right-hand) side of the plot. This arc is due to the interface between the ionically conducting sample and the electronically conducting electrode, and is not a response of the bulk cement paste. The bulk arc to the left of the electrode arc is the response of the paste. The point where the bulk and electrode arcs intersect on the real axis ( $\sim 470 \Omega$  on Fig. 1) is the bulk resistance of the sample, and is equivalent to the d.c. resistance of the sample. The separation of bulk and electrode effects in IS is a much more reliable way of measuring the true d.c. resistance than single-frequency electrical measurements. Higher frequency measurements that would be located to the left of those shown in Fig. 1 are currently unattainable, owing to experimental limitations, which make the maximum reliable frequency to be about 3 MHz [2].

While initial efforts to explain IS spectra in terms of microstructure have had some success [4–13], some implications of the experimental results have been hard to reconcile with prevailing theories of microstructural development. The purpose of this paper is to explain these puzzling features, described below, using a computer model.

## 2. Puzzling experimental features

The conductivity of cement paste may be described by a simple effective medium equation [14]

$$\sigma = \sigma_0 \beta V_f, \quad (1)$$

where  $\sigma$  is the composite conductivity,  $\sigma_0$  is the conductivity of the capillary porosity, by far the most conductive phase in cement paste,  $V_f$  is the volume fraction of the capillary porosity, and  $\beta$  is a microstructural parameter related mainly to the tortuosity and connectivity of the capillary porosity, and to a lesser extent to the tortuosity and connectivity of the C-S-H phase. Normalizing the composite conductivity  $\sigma$  by  $\sigma_0$ , leaves  $\beta V_f$ , which is a measure of the influence of the microstructure on the composite conductivity. The parameter  $\beta$  is an empirical constant related to the arrangement and relative amounts and conductivities of the conductive phases, and can only be analytically calculated for simple microstructures. For example, Fig. 2 shows a plot of normalized con-

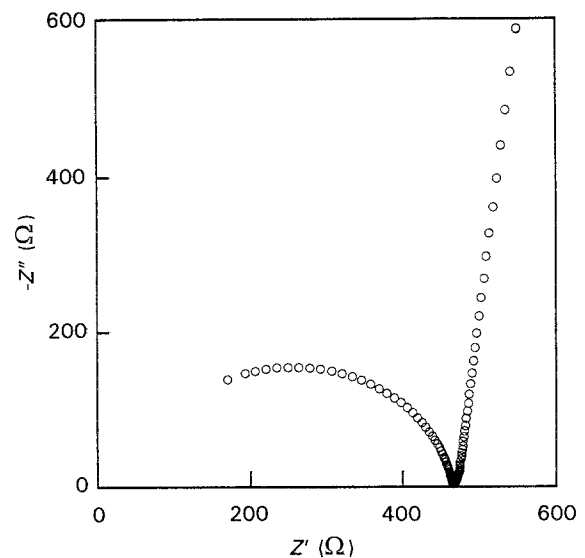


Figure 1 Nyquist plot of a  $C_3S$  paste with water to cement ratio of 0.45, reacted for 14 days.

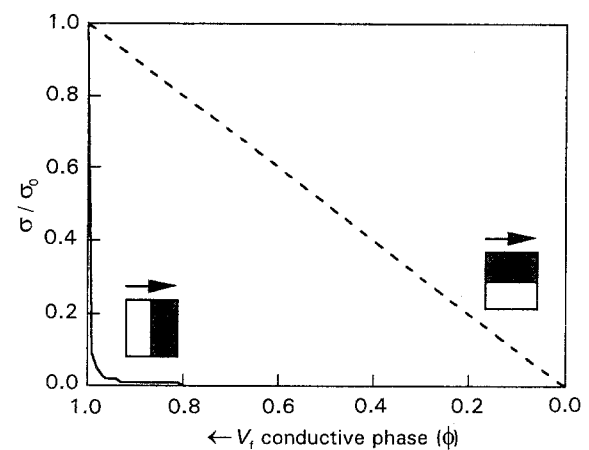


Figure 2 The composite conductivity of (---) parallel and (—) series composite microstructures. The conductivity has been normalized by the conductivity of the more conducting phase. The two phase conductivities differ by three orders of magnitude.  $V_f$  is the volume fraction of the higher conductivity phase.

ductivity,  $\sigma/\sigma_0$ , versus volume fraction of the more conductive phase,  $V_f$ , for two simple two-phase microstructural arrangements. In these examples, the conductivity of the two phases differ by a factor of 1000. In Fig. 2, the straight, dashed line represents a parallel arrangement of the two phases, while the lower solid curve represents a series arrangement. As can be seen in the figure,  $\beta$  for the parallel case is 1, while for a series arrangement,  $\beta$  drops to a very low value as soon as the resistive phase is present. It is also important to note that for any two conducting-phase material, the conductivity of the parallel and series arrangements are strict upper and lower bounds for the true composite conductivity [15].

Fig. 3 is a semi-log plot of the data in Fig. 2, together with conductivities for two cement pastes with different water to cement ratios and various degrees of reaction, normalized by their pore fluid conductivities. (The fraction of capillary porosity is calculated from the degree of reaction using the Powers–Brownyard model [16]. The composite conductivity,  $s$ , is obtained directly from the bulk resistance by correcting for the sample geometry, and the

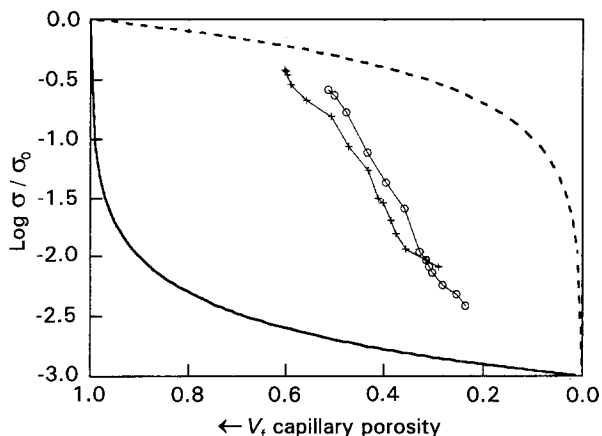


Figure 3 Normalized conductivity data for two ordinary portland cements with different water to cement ratios, w/c: (+) 0.50, (o) 0.35. (---) Parallel and (—) series bounds, shown in Fig. 2.

conductivity of the pore fluid,  $\sigma_0$ , is measured directly after extracting it from the paste samples.) If the amount of “parallel” or “series” character of the material is defined by the point at which a conductivity data point lies between the parallel and series bounds, then it appears that the cement paste microstructure is making a transition from having a mostly parallel character at high volume fractions of porosity, to having a mostly series character at low volume fractions of porosity. The capillary pore space is clearly losing connectivity and volume, while it is filled in with reaction products, thus leading to the observed drop in composite conductivity. This transition points to an eventual depercolation of the capillary porosity, but depercolation, or loss of connectivity is neither observed by other techniques [16], nor predicted by percolation theory [17], nor computer simulation [18], until a volume fraction near 20%. A disconnected capillary pore space would, of course, display series character as current flows through the (always) connected C–S–H and through the isolated capillary pores.

A series character in the microstructure at porosity volume fractions greater than 20% may also be indicated by the full Nyquist plot, according to the following argument. Fig. 4 shows the impedance spectrum of Fig. 1, with the bulk arc fitted by a semicircle whose centre is depressed below the axis. The parameters  $n$  and  $Q$  come from fitting the arc with a “constant phase element”, which becomes a perfect capacitor in parallel with a perfect resistor when  $n = 1$  [2, 3]. Fig. 4 shows that the fitted arc, when extended to frequencies higher than those measured, does not extend to zero impedance, but rather to some real resistance greater than zero, defined as an “offset resistance” [4].

This behaviour is unexpected, because the conductive pore phase is almost certainly well connected for a sample with this initial water:cement ratio (0.45) and age of reaction (14 days). The impedance of a pure capacitor is inversely proportional to frequency

$$Z_{\text{capacitor}} = -i/\omega C, \quad (2)$$

where  $\omega$  is the applied angular frequency,  $C$  is the capacitance of the capacitor, and  $i$  is the square root

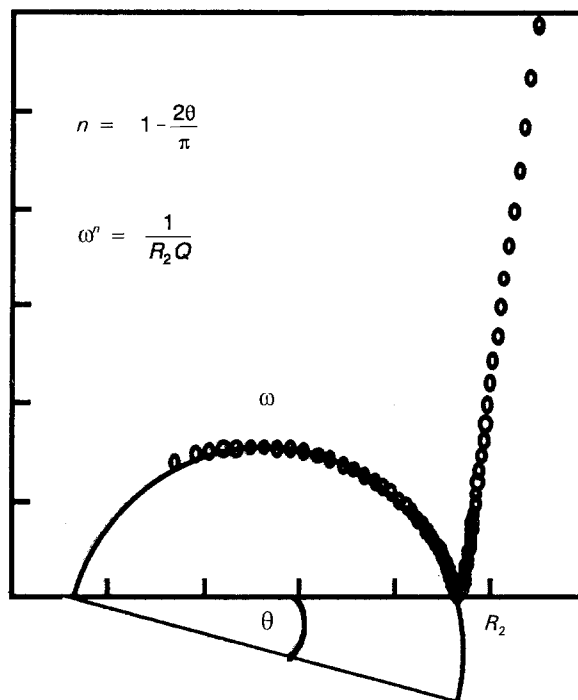


Figure 4 Impedance arc analysis used to determine effective dielectric constant, bulk resistance, and offset resistance. The parameters  $n$ ,  $Q$ , and  $\omega$  are explained in the text.

of  $-1$ . Thus, for an ideal connected phase,  $Z_{\text{capacitor}}$  approaches zero as the applied frequency becomes infinite. Because the C–S–H phase is always connected, from a few hours of hydration on, and because the C–S–H phase has a capacitive character [2], this implies that the arc must eventually go to the origin. Therefore, there must be a second arc, unseen by experiment because its frequency is beyond experimental limits.

The models usually used to analyse impedance spectra are simple series and parallel combinations of resistors and capacitors [3]. Series behaviour results in two arcs as seen in Fig. 5, where two RC circuits arranged in parallel and series are shown, along with their impedance spectra. Thus, according to this analysis, the electrical properties of cement paste are behaving as if the conducting phases were assembled in series, which would imply that the capillary pore space is disconnected. Because of the low resistance of freshly mixed pastes, arising from the high conductivity of the pore fluid, an impedance arc cannot be observed at very early times, as most of the arc is at frequencies too high to be observed experimentally. However, enough of an arc to be analysed can be observed at times that are still early enough so that the capillary pore space is almost certainly still percolated [2]. Even at early hydration times, where the volume fraction of capillary porosity can be 40% or more, it appears that an offset resistance may be present.

Both aspects of the impedance spectrum described above indicate that the phases within the composite are arranged to some extent in a series manner. In other words, the microstructure must have some series character. Because the pore fluid is the most conductive phase in the microstructure, the series behaviour

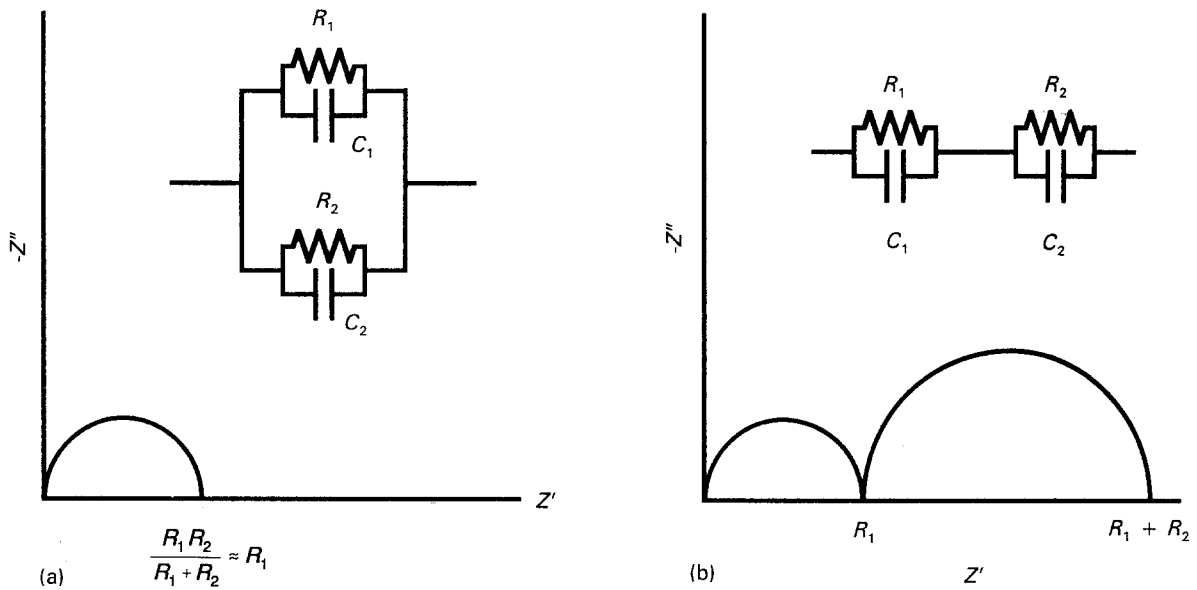


Figure 5 Impedance response for equivalent circuits arranged in (a) parallel and (b) series.

implies, according to the usual models used to analyse IS, that the pore fluid is disconnected at volume fractions for which most other information indicates otherwise.

However, it has recently been shown that two-arc behaviour, for a composite with two conducting phases that can differ greatly in conductivity, can be manifested when either both phases are connected, or when the lower conductivity phase is disconnected [19]. This perhaps unexpected result can analytically be seen to be true by considering the dilute (small inclusion volume fraction  $c_2$ ) limit of the Maxwell–Garnett equation, for a composite made up of a matrix material and spherical inclusions [3]

$$\sigma = \sigma_1 + 3c_2(\sigma_2 - \sigma_1)/(2\sigma_1 + \sigma_2), \quad (3)$$

where  $\sigma$  is the composite conductivity,  $\sigma_1$  is the complex matrix conductivity, and  $\sigma_2$  is the complex inclusion conductivity. When the inclusion volume fraction is small, Equation 3 gives the exact behaviour of the composite conductivity. When the phase parameters are chosen so that the inclusions have a significantly different peak frequency response than the matrix, the exact conductivity, displayed in a Nyquist plot, displays a two-arc behaviour [19]. An example is shown in Fig. 6, with the conductivities and volume fractions given in the caption. The peak frequencies for both arcs are marked on the figure, and the axes are in arbitrary resistance units. The main current paths will, of course, go around the isolated inclusions, because the inclusions have a lower conductivity than the matrix, but there will always be some current going from the matrix, through the spherical inclusions, and back into the matrix, because this is a shorter distance than going around the inclusions. Any current which flows across a phase interface means that some series behaviour will be displayed, and so two arcs will be observed if the peak frequencies for the two phases differ sufficiently. This simple analytical example shows how tortuosity (non-straight line current paths) can produce series-like two-arc behaviour.

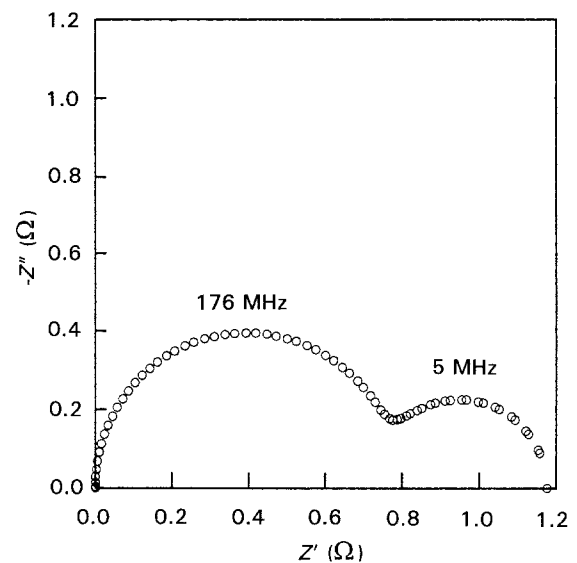


Figure 6 Graph of Equation 3, plotting the imaginary part of the impedance versus the real part. The phase complex conductivities were chosen to be  $\sigma_1 = 1.0 + 100i$ ,  $\sigma_2 = 0.001 + 5000i$ , and the volume fraction of phase 2 was chosen to be 0.1. The units are such that  $E_0 = 1$ , so that the low-frequency dielectric constant of phases 1 and 2 are 100 and 5000, respectively.

### 3. Description of the computer model

To understand better the apparent series behaviour of hydrating cement pastes, a computer model was used to demonstrate that a tortuous pore phase is responsible for the observed series-like behaviour. A model that computes impedance spectra from digital representations of microstructure in two or three dimensions has been developed [19]. Each discrete element (pixel) in an array is considered to be a single, homogeneous phase. The impedance properties of all the pixels are then summed to give an overall composite response for this microstructure. Garboczi and Bentz [20] have published a complete review of this type of microstructural representation of cement paste. The ability of this model to reproduce quantitatively

experimental IS curves from a simulated microstructure of cement paste provides a powerful tool in establishing structure-property relationships, especially concerning a.c. electrical properties.

The microstructural development of cement paste during hydration was simulated using the Bentz-Garbocki  $C_3S$  hydration model [21]. Images used for this model are typically  $100^3$  pixels, where each pixel is a cube of volume  $1 \mu\text{m}^3$ . The cement particle-size distribution used in these simulations consists of ten different sizes, and was taken from a measured distribution of  $C_3S$  powder. This distribution was used in all the models presented here. The computer resources needed to implement the impedance computation on a  $100^3$  image are significant, and require the use of a supercomputer for both memory and processing time. Because supercomputer resources were limited, smaller  $50^3$  models, which can be executed on various high-performance workstations, were used to explore general trends and to establish initial phase parameters.

A measure of the connectivity of the pore phase (and other phases) is readily achieved in the simulated microstructures by using a "burning" algorithm [18]. The burning algorithm propagates a "fire" throughout the microstructural phase being assessed. If the fire reaches the opposite side from which it was started, the phase is percolated in that particular direction. This technique was employed on all the microstructures used in this study to determine if the pore-fluid phase was connected in the direction of the applied voltage. For systems of both sizes ( $50^3$  and  $100^3$ ) and several different water to cement ratios, the percolation threshold of pore-fluid phase occurred when its volume fraction fell slightly below 20%. This is consistent with the 18% value determined from the same model previously using a different cement particle-size distribution [18], implying that the capillary porosity percolation threshold is fairly insensitive to cement particle-size distribution.

The impedance of the model is computed by solving the complex Laplace's equation for a random, complex conductor [3]. A node is placed in the middle of each pixel, and an RC (a resistor in parallel with a capacitor) element is connected between each node, with the value of  $R$  and  $C$  determined by the local complex conductivity for the phase occupying that pixel. Electrodes are added to either side of the microstructure image, and "wired" into the network. A single-frequency voltage is then applied, and the complex Kirchoff's laws are solved for the network using a conjugate gradient method. Details are given elsewhere [19]. The total current in the network, divided by the applied voltage, then defines the impedance.

Before implementing the impedance simulation, it was necessary to estimate the impedance properties of the individual phases, in order to be able to define the local RC elements to be used. Once reasonable estimates were obtained, these parameters were modified to achieve the best fit with the experimental data. Especially important are the properties of the pore fluid and C-S-H, because these phases are the most abundant and are considered the most important in determining the electrical properties of cement paste.

The conductivity of pore fluid was determined experimentally by direct measurement after being extracted from cement paste, and is in the range of  $1-10 \text{ S m}^{-1}$  [5]. It is assumed that pore fluid from  $C_3S$  pastes is not as conductive as that of Portland cement paste because of the absence of alkali ions [5]. The conductivity of saturated CH (lime) solution was found to be  $2 \text{ S m}^{-1}$ , which is taken in the model for simplicity as  $1 \text{ S m}^{-1}$ . Because the number ultimately to be computed is the composite conductivity, normalized by the pore-fluid conductivity, an overall multiplicative factor in the pore-fluid conductivity will not affect results. Because the pore fluid is highly conductive, its dielectric constant is not directly measurable by the impedance technique, because not enough of an arc can be generated to analyse, as was mentioned above, and so is assumed to be that of water,  $k_r = E/E_0 = 80$  [22]. Some experimental results have put an upper bound of approximately 150 on the value of  $k_r$  [2].

Previous results from a d.c. simulation [23] indicated that the conductivity of C-S-H was about 400 times less than pore fluid. The first estimate of the dielectric constant of C-S-H is based on measurements for synthetic C-S-H and completely hydrated samples that used silica fume to produce a material that is mostly C-S-H [2]. These measurements indicate that the relative dielectric constant of C-S-H is at least several times higher than that of pore fluid. Also, because C-S-H is probably a layered structure [1], with pore fluid residing to some extent in between the solid layers, it is reasonable to expect that its dielectric constant is larger than that of pore fluid, perhaps significantly larger, amplified due to a fluid-solid layering effect [3]. The subject of dielectric amplification as it occurs in C-S-H, and in cement paste itself, will be discussed in Part II of this paper [24]. Because both  $C_3S$  and CH are known to be insulators, they are assumed to have very low conductivities and low dielectric constants. In the model, the dielectric constants for CH and  $C_3S$  were chosen to be 1 for simplicity. Other results, not presented here, indicate more realistic values for dielectric constant ( $\sim 5$ ) have

TABLE I Model parameters

| Phase      | Initial values,<br>$\sigma (\text{S m}^{-1})$ | Initial values,<br>$k_r$ | Final values,<br>$\sigma (\text{S m}^{-1})$ | Final values,<br>$k_r$ |
|------------|---|--------------------------|---|------------------------|
| Pore fluid | 1.75  | 80                       | 1.0   | 80                     |
| C-S-H      | 0.004375                                      | 1000                     | 0.01  | 500                    |
| $C_3S$     | $3.6 \times 10^{-8}$                          | 1                        | $3.6 \times 10^{-8}$                        | 1                      |
| CH         | $3.6 \times 10^{-8}$                          | 1                        | $3.6 \times 10^{-8}$                        | 1                      |

no effect on the composite response. Columns 2 and 3 of Table I show the initial parameters used in the model for a large number of the  $50^3$  systems.

#### 4. Results

Fig. 7 shows a comparison of the normalized conductivity data presented in Fig. 3 with results from a number of  $50 \times 50 \times 50$  models. The models include several different water to cement ratios and degrees of reaction. Although the model overpredicts the conductivity at lower volume fractions of porosity, it shows similar trends to experimental values, in agreement with earlier simulations [25]. The important point is that in the model, the capillary porosity has not lost long-range connectivity in any of the microstructures until below about 20%. Therefore, the transition from parallel to series behaviour seen in the experimental results is obtainable in a tortuous, yet connected, conductive phase. The results from the model can be adjusted to better match the experimental curves in Fig. 7 by decreasing the (unknown) conductivity of the C-S-H phase with respect to that of the (known) pore-fluid conductivity. However, it is possible that the overprediction of conductivity is at least partially an artefact of the finite resolution of the digital-image model. Because the distribution of porosity in the model is limited to quantized units of  $1 \mu\text{m}^3$ , the same amount of porosity in the model will be distributed in fewer, larger pores than probably exist in cement paste. It is known that capillary pores can be smaller than  $1 \mu\text{m}$  [1]. Simple models have shown this latter type of distribution to have a somewhat higher conductivity at the same total porosity [13].

Even though the model parameters listed in columns 2 and 3 of Table I provide a good fit to the normalized zero-frequency conductivity data shown in Fig. 7, they must be modified slightly to obtain a better rounded fit to the impedance response at all frequencies. To achieve the best overall fit with experimental results, systems of similar water to cement ratios and degrees of reaction were compared. Because model and experimental geometries are different, the

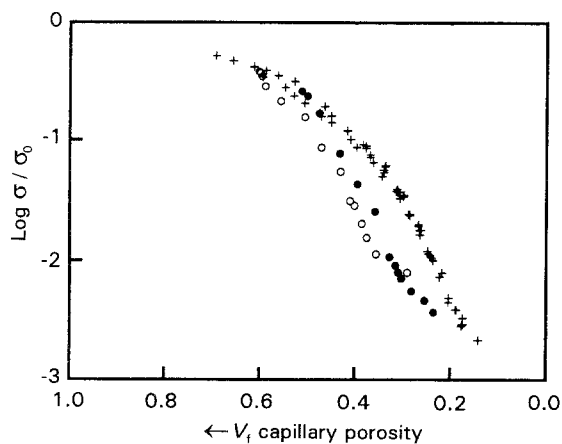
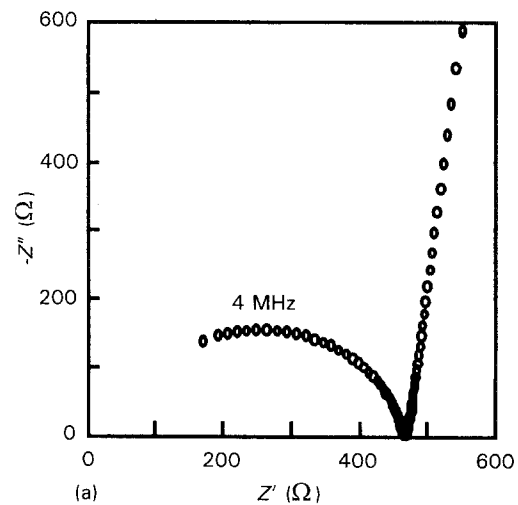


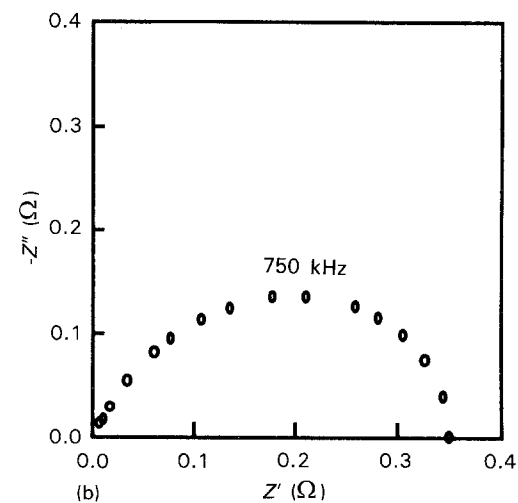
Figure 7 Comparison of normalized conductivity from experiment and simulation for various water to cement ratios: (o) OPC 50, (+) model, (●) OPC 35.

following three aspects of the IS curves were used to compare and modify the model values: normalized conductivity; dielectric constant as measured by EQUIVCRT [26], a commercial impedance spectra analysis software package; and the arc peak frequency, which is the frequency at which the imaginary part of the impedance,  $-Z''$ , takes its maximum value. Each of these parameters is sample-geometry independent [27].

Fig. 8b shows a simulated curve from a  $100^3$  pixel model whose parameters have been modified to match closely the accompanying experimental curve in Fig. 8a. The simulated spectrum goes to the origin at high frequencies as predicted, and the shape of the arc at high frequencies (left side of the curve) shows the presence of another arc, which, however, is not well separated from the main arc for this fairly high degree of reaction paste. The model parameters used in Fig. 8 are given in columns 4 and 5 of Table I. Fig. 8b does not show an electrode arc. It is possible to simulate such an arc, by placing an RC element between the simulated electrode and microstructure [13], but the data that make up the electrode arc are not relevant to the response of the microstructure. To make certain of



(a)



(b)

Figure 8 Comparison of impedance arcs from (a) experiment and (b) simulation. (a)  $\alpha \approx 0.55$ ,  $\sigma/\sigma_0 = 0.02$ ,  $k_r = 1300$  (b)  $\alpha = 0.51$ ,  $\sigma/\sigma_0 = 0.03$ ,  $k_r = 1200$ .

this, a few cases were run with and without the electrode arc. It was found that omission of the electrode arc had a negligible effect on the response of the microstructure and the computed bulk resistance. This result was also found previously in two-dimensional models [13]. Electrode arcs were thus not usually simulated, in order to conserve limited super-computer resources.

The impedance curves displayed in Fig. 9a and b were generated by the model and represent the evolution of a single  $100^3$  system as the hydration reaction proceeds. The phase parameters used for these simulations are given in the fourth and fifth columns of Table I. The fitted semicircle present in Fig. 9b exhibits the offset resistance that would be observed if the right-hand side of the arc were fitted with an equivalent circuit at experimentally observable frequencies. The simulated spectra, as in Fig. 8b, also go to the origin at high frequency. At smaller degrees of hydration (earlier hydration times), the two-arc beha-

viour is clearly displayed. As the amount of pore fluid is decreased, the higher frequency arc diminishes, leading to the identification of the low-frequency arc as being due primarily to C-S-H, and the diminishing higher frequency arc being due primarily to the remaining pore fluid. The model indicates that there is then no true offset resistance, but rather a second arc corresponding to the pore-fluid phase. As the pore fluid is replaced with more resistive reaction products, the bulk resistance increases, and the pore-fluid arc is less noticeable. Because it is known that the pore fluid is percolated in the first three of the four microstructures analysed in Fig. 9 ( $\alpha = 0.229, 0.314, \text{ and } 0.505$ ), it is clear that the observed behaviour in the impedance curves is a result of tortuous, but connected, pore-fluid phase that is intertwined with continuous conduction paths of C-S-H.

In general, the behaviour of the simulated IS curves is the result of a composite response of the microstructure, which depends only on the properties of the individual phases and their arrangement within the microstructure. The response is not dependent on any special interaction or interfaces between the phases, because reasonable agreement between experiment and simulation was obtained without any such interactions or interfaces being simulated. The origin of the bulk arc has been attributed by other researchers [12, 28] to electrical double layers that form on surfaces that develop in the microstructure of cement paste. This hypothesis has significant ramifications with respect to the effective dielectric constant of the bulk arc, and will be discussed further in Part II [24] of this paper.

## 5. Conclusions

With the proper selection of electrical properties for the microstructural phases, the impedance spectrum of cement paste can be quantitatively modelled. Results from the model suggest that the changes in the impedance spectra that accompany hydration are due to changing amounts, distribution, and arrangements of phases. The main features of the impedance spectrum of cement paste result from a composite response of microstructural phases and are not the result of interactions or interfaces between these phases.

The decrease in normalized conductivity that accompanies the hydration reaction can be explained by an increase in the tortuosity of the capillary pore structure without requiring a premature disconnection, or depercolation, of porosity. The tortuosity of the capillary pore structure, intertwined with the conducting C-S-H phase, can also give rise to two-arc behaviour. The model indicates the existence of a high-frequency arc due to the response of pore fluid, which had been interpreted previously as an offset resistance [4-12]. The high-frequency behaviour of the impedance spectrum is better explained by the existence of a second arc, rather than a series arrangement of the conducting phases giving rise to an offset resistance with physical meaning.

Fitting the model to experimental results by varying the electrical parameters of the various phases leads to

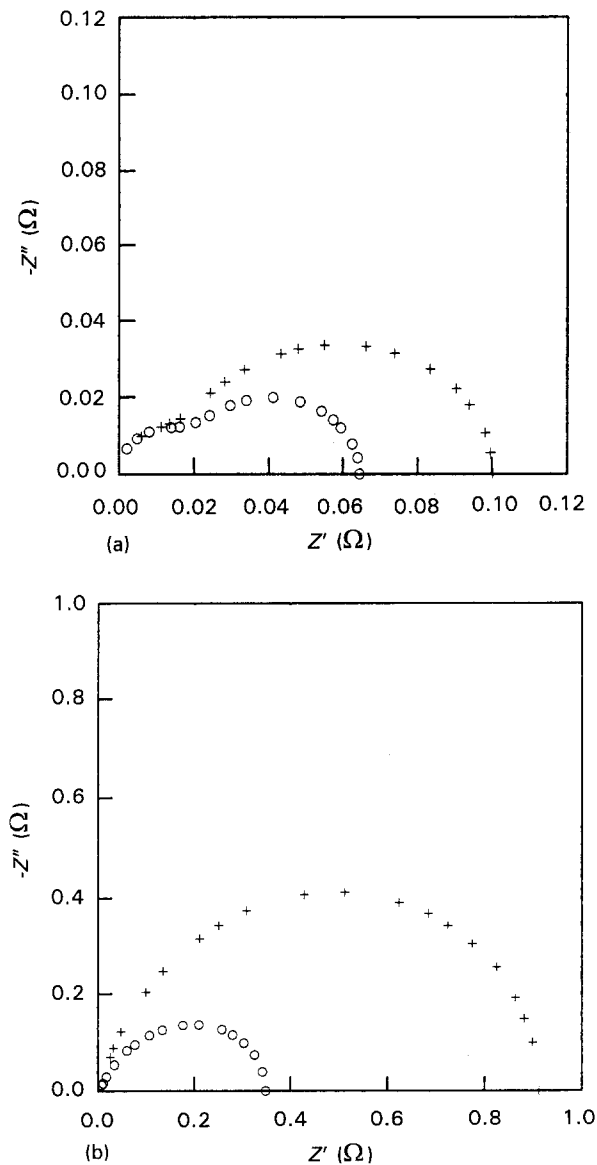


Figure 9 Simulated impedance curves for a single  $100 \times 100 \times 100$  system with a water to cement ratio of 0.4; (a)  $\alpha = 0.229$ , (+) 0.314 and (b)  $\alpha = 0.505$ , (+) 0.650. Note change of scale between (a) and (b).

the conclusion that C-S-H has a relative dielectric constant of the order of 500, and a conductivity approximately 100 times smaller than pore fluid. This conductivity is obviously expected to scale with pore-fluid conductivity, as C-S-H probably derives its conductivity from having its nanometre-scale pores filled with conductive pore solution.

Finally, the use of microstructure models, accompanied by accurate computations of properties such as impedance spectra, allows the researcher to go beyond simple series and parallel ideas, enabling more quantitative and detailed understanding of microstructure-electrical property relationships to be achieved.

### Acknowledgements

The authors acknowledge the National Science Foundation's Center for Science and Technology for Advanced Cement Based Materials, under grant number DMR-08432, for financial support. Supercomputing facilities were provided by the National Center for Super Computing Applications at the University of Illinois at Champaign-Urbana, under grant number DMR-920024N.

### References

1. H. F. W. TAYLOR, *Cement Chemistry* (Academic Press, London, 1990) p. 1.
2. B. J. CHRISTENSEN, PhD thesis, Northwestern University (1993).
3. J. R. MACDONALD and W. B. JOHNSON, in "Impedance Spectroscopy: Emphasizing Solid Materials and Systems", edited by J. R. MacDonald (Wiley, New York, 1987) pp. 12-26.
4. C. A. SCUDERI, T. O. MASON and H. M. JENNINGS, *J. Mater. Sci. Lett.* **7** (1988) 1056.
5. B. J. CHRISTENSEN, T. O. MASON and H. M. JENNINGS, *J. Am. Ceram. Soc.* **75** (1992) 939.
6. P. GU, Z. XU, P. XIE and J. J. BEAUDOIN, *Cem. Conc. Res.* **23** (1993) 531.
7. Z. XU, P. GU, P. XIE and J. J. BEAUDOIN, *ibid.* **23** (1993) 853.
8. *Idem*, *ibid.* **23** (1993) 1007.
9. P. GU, P. XIE and J. J. BEAUDOIN, *ibid.* **23** (1993) 581.
10. P. GU, P. XIE, J. J. BEAUDOIN and R. BROUSEAU, *ibid.* **22** (1992) 833.
11. *Idem*, *ibid.* **23** (1993) 157.
12. P. XIE, P. GU, Z. XU and J. J. BEAUDOIN, *ibid.* **23** (1993) 359.
13. R. T. COVERDALE, E. J. GARBOCZI, B. J. CHRISTENSEN, T. O. MASON and H. M. JENNINGS, *J. Am. Ceram. Soc.* **76** (1993) 1153.
14. E. J. GARBOCZI, *Cem. Conc. Res.* **20** (1990) 591.
15. Z. HASHIN, *J. Appl. Mech.* **50** (1983) 481.
16. T. C. POWERS and T. L. BROWNYARD, *Proc. ACI* **43** (1947) 865.
17. R. ZALLEN, "The Physics of Amorphous Solids" (Wiley, New York, 1983) Ch. 4.
18. D. P. BENTZ and E. J. GARBOCZI, *Cem. Conc. Res.* **21** (1991) 325.
19. R. T. COVERDALE, E. J. GARBOCZI and H. M. JENNINGS, *J. Computat. Mater. Sci.*, to be submitted.
20. E. J. GARBOCZI and D. P. BENTZ, in "Materials Science of Concrete II", edited by J. Skalny and S. Mindess (American Ceramic Society, Westerville, OH, 1991) pp. 249-77.
21. E. J. GARBOCZI and D. P. BENTZ, *Ceram. Trans.* **16** (1991) 211.
22. J. R. HASTED, "Aqueous Dielectrics" (Chapman and Hall, London, 1973) p. 137.
23. E. J. GARBOCZI and D. P. BENTZ, *J. Mater. Sci.* **27** (1992) 2083.
24. R. T. COVERDALE, B. J. CHRISTENSEN, T. O. MASON, H. M. JENNINGS, E. J. GARBOCZI and D. P. BENTZ, *J. Mater. Sci.*, in press.
25. B. J. CHRISTENSEN, T. O. MASON, H. M. JENNINGS, D. P. BENTZ and E. J. GARBOCZI, in "Advanced Cementitious Systems: Mechanisms and Properties", edited by F. P. Glasser, G. J. McCarthy, J. F. Young, T. O. Mason and P. L. Pratt, Symposium Proceedings Vol. 245 (Materials Research Society, 1992) pp. 259-64.
26. B. A. BOUKAMP, "Equivalent Circuit (EQUIVCRT.PAS)", University of Twente, Department of Chemical Technology, P.O. Box 217, 7500 AE Enschede, The Netherlands (1988).
27. R. T. COVERDALE, PhD thesis, Northwestern University (1993).
28. W. J. McCARTER, S. GARVIN and N. BOUZID, *J. Mat. Sci. Lett.* **7** (1988) 1056.

Received 18 January  
and accepted 21 March 1994